



Residual stress analysis of energy-dispersive diffraction data using a two-detector setup: Part I — Theoretical concept



Daniel Apel^{a,*}, Matthias Meixner^a, Alexander Liehr^b, Manuela Klaus^a, Sebastian Degener^b, Guido Wagener^a, Christian Franz^b, Wolfgang Zinn^b, Christoph Genzel^a, Berthold Scholtes^b

^a Helmholtz-Zentrum Berlin für Materialien und Energie, Berlin, Germany

^b Universität Kassel, Kassel, Germany

ARTICLE INFO

Keywords:

X-ray residual stress analysis
Energy-dispersive diffraction
Two-detector setup

ABSTRACT

A new goniometer setup for energy-dispersive X-ray diffraction is introduced which is based on simultaneous data acquisition with two detectors D1 and D2, both of them freely movable in a horizontal as well as in a vertical plane. From the multitude of measurement configurations that can be realised with this setup, we figured out three efficient concepts which aim at the fast analysis of residual stress depth profiles by combining the diffraction data gathered with the two detectors. The characteristic feature of the first two configurations consists in the vertical (horizontal) positioning of the first (second) detector, which results in a diffraction geometry where the two scattering vectors span a plane that coincides with the X-circle used for sample tilt. Because each detector does see the sample under another viewing angle, both the positive and the negative ψ -branch are covered by just one χ -tilt between 0° and 90° (configuration 1) and 0° and 60° (configuration 2), thus allowing for the simultaneous analysis of the in- and out-of-plane residual stress depth gradients $\sigma_{ii}(\tau)$ and $\sigma_{i3}(\tau)$ ($i = 1, 2$), respectively, from data sets $d_{D1}^{hkl}(\chi)$ and $d_{D2}^{hkl}(\chi)$. The third configuration introduced in this paper is based on a ϕ -rotation of the sample under a constant tilt angle χ and enables a fast and reliable tracing of shear stress fields $\sigma_{i3}(\tau)$ ($i = 1, 2$).

© 2017 Elsevier B.V. All rights reserved.

1. Introduction

The analysis of residual stress fields in the near-surface region of polycrystalline materials and thin films plays an important role in order to quantify and understand the impact of manufacturing and processing on the materials properties. Surface processing steps like grinding, shot-peening, hardening, turning or the deposition of coatings are well known to induce complex residual stress fields in the polycrystalline materials near-surface region, which often is characterised by a pronounced depth dependence [1–3]. During the past decades, various concepts and experimental methods based on angle-dispersive (AD) and energy-dispersive (ED) diffraction have been developed and successfully applied to phase specific and non-destructive X-ray stress analysis (XSA) (see, for example, the summaries by (Hauk [3]; Genzel [4]; Welzel et al. [5]; Reimers et al. [6]; Spiess et al. [7]; Mittemeijer & Welzel [8]). Based on the definition of an average information depth $\langle z \rangle$ to which the information extracted from the diffraction lines has to be ascribed, the different methods can be divided into the ‘real space’ and the ‘Laplace space’ methods [9].

The real space methods are based on the definition of a gauge volume by narrow slits in the primary as well as in the diffracted beam. By scanning the gauge volume under one or more orientations into or within the sample, strain or stress depth profiles can be obtained [10–14]. Other real space approaches exploit the high resolution provided by the micro- and nanobeam techniques being available at modern 3rd generation synchrotron sources [15,16] and allow for lattice strain and residual stress analysis as a direct function of the depth z in thin slices of sample cross sections prepared from multi-layer coating systems [17–19].

In contrast, the Laplace space methods make use of the exponential attenuation of X-rays by matter, as described by Beer–Lambert’s law. Here, depth resolution is achieved by the stepwise variation of tilt ($\sin^2\psi$ -based approaches, see e.g., [20–22] or rotation angles (scattering vector method, see [23]), leading to a continuous variation of the so called $1/e$ information depth τ . Other techniques like the low-incidence beam angle diffraction method [24,25] and related methods [26–28] and the so-called $\Omega - \Psi$ method [29–31] control the information

* Corresponding author.

E-mail address: daniel.apel@helmholtz-berlin.de (D. Apel).

depth *via* the incidence angle α or appropriate angle sets (φ, ψ) (mixed-mode technique) and allow for residual stress analysis at predefined average information depths. As a consequence of the exponential beam attenuation, all strain and residual stress depth distributions obtained from such experiments are profiles in the Laplace space, $\varepsilon(\tau)$ and $\sigma(\tau)$, respectively. The corresponding real space profiles $\varepsilon(z)$ and $\sigma(z)$ can be accessed by applying the inverse Laplace transform. Because numerical approaches fail in most cases [32], it has become common practice to describe the depth profiles $\varepsilon(z)$ and $\sigma(z)$ using polynomial [33] and exponentially damped [34] functions which can be easily transformed into the Laplace space and fitted to the discrete Laplace stress data using a least-squares method. A comparative assessment of the Laplace and real space methods has been reported by Stefanelli et al. [35].

In the recent past the ED diffraction method increasingly gained application for the analysis of near-surface residual stress and structure gradients. The advantage of the ED mode compared to the AD mode of diffraction is that it yields complete diffraction spectra with a multitude of diffraction lines in a fixed but arbitrary measuring direction. Additionally, each of the individual diffraction lines E^{hkl} in the ED diffraction spectrum can be assigned to a specific information depth, allowing for a depth resolved analysis of structure gradients [36–39]. The development of new areas of application and a wider distribution of the ED mode of diffraction, as it would be adequate for the high potential of this method, is in contrast to the limited availability of appropriate synchrotron radiation sources and beamlines.

The first part of this two-part series aims at introducing concepts for depth resolved residual stress analysis of polycrystalline materials, which exploit the feature of ED diffraction to provide diffraction patterns in arbitrary scattering directions simultaneously. The approaches are designed for a two-detector setup and require a special diffractometer system that must be equipped with flexible sample and detector positioning units. The latter must allow for independent movements of both detectors in the horizontal as well as in the vertical plane. In the first part we address the measurement configurations and the data evaluation concepts by means of simulated examples from a more theoretical point of view. Part two is dedicated to real experimental examples measured with the Bremsstrahlung emitted by a conventional tungsten X-ray tube on an 8-circle diffractometer which fulfils the above requirements. It should be emphasised that the diffractometer system introduced in the second part could be operated as experimental station for residual stress analysis at any synchrotron beamline running in the ED diffraction mode as well. However, against the background of the limited availability of synchrotron beamtime we are of the opinion that its main application area will be that of a stand-alone instrument operated with a lab X-ray source. With the examples shown in both parts of the series we will demonstrate that the data evaluation methods based on the additional information gained simultaneously by the second detector are matched to the terms of a lower photon flux.

2. Fundamental aspects of $\sin^2\psi$ -based energy-dispersive near-surface residual stress gradient analysis

Exploiting ED diffraction to analyse near-surface residual stress gradients entails significant advantages compared to AD diffraction. Residual stresses are not directly accessible by means of diffraction methods but they are analysed by means of measuring the associated lattice strains $\varepsilon_{\varphi\psi}^{hkl}$. These strains result from the variation of the distance $d_{\varphi\psi}^{hkl}$ between the crystallographic lattice planes hkl compared to the respective strain-free lattice spacing d_0^{hkl} . Using the continuous energy spectrum of a white beam X-ray source, it is possible to detect the shifts of multiple diffraction lines hkl for different angle sets (φ, ψ) of the scattering vector $g_{\varphi\psi}^{hkl}$ simultaneously. In the case of ED diffraction the relation between the lattice spacing d^{hkl} and the corresponding diffraction line E^{hkl} on the energy scale is given by [40]

$$d^{hkl} (\text{\AA}) = \frac{6.199}{\sin \theta} \frac{1}{E^{hkl} (\text{keV})}. \quad (1)$$

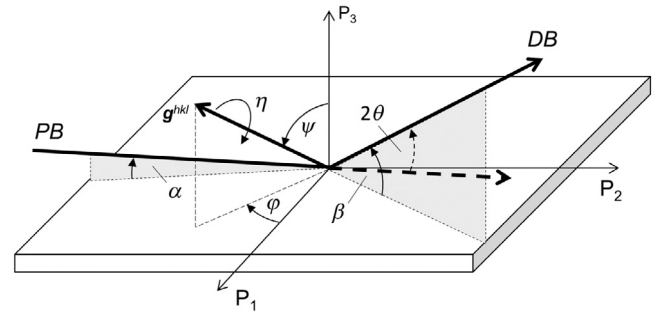


Fig. 1. Diffraction geometries in X-ray stress analysis. \mathbf{P} denotes the sample reference system, α and β are the incidence and the exit angle formed by the primary (PB) and the diffracted beam (DB), respectively, and the sample surface. The “sampling angles” φ and ψ define the orientation of the scattering vector g^{hkl} (in Figs. 2, 3 and 5 denoted by $S1$ and $S2$) within the sample reference system, whereas η describes the rotation of the sample around g^{hkl} , which is used to vary the information depth τ .

The value 6.199 in the above equation originates from the term $hc/2$ with h and c being Planck’s constant and the speed of light, respectively. The Bragg and the diffraction angle, θ and 2θ , respectively, can be selected freely but remain fixed during the experiment. Considering Eq. (1), the lattice strain $\varepsilon_{\varphi\psi}^{hkl}$ determined for an angle set (φ, ψ) with respect to the sample reference system becomes

$$\varepsilon_{\varphi\psi}^{hkl} = \frac{d_{\varphi\psi}^{hkl}}{d_0^{hkl}} - 1 = \frac{E_0^{hkl}}{E_{\varphi\psi}^{hkl}} - 1 \quad (2)$$

where E_0^{hkl} denotes the energy that corresponds to the strain-free lattice spacing d_0^{hkl} . The information depth τ^{hkl} corresponding to each diffraction line E^{hkl} can be expressed by

$$\tau^{hkl} = \frac{1}{\mu(E^{hkl})k} = \frac{\sin \alpha \sin \beta}{\mu(E^{hkl})(\sin \alpha + \sin \beta)} \quad (3)$$

where $\mu(E)$ is the energy-dependent linear absorption coefficient and α and β denote the angles which are formed by the primary and secondary beam with the sample surface (see Fig. 1). For any diffraction geometry the angles α and β can be expressed as a function of the Bragg-angle θ , the inclination angle ψ between the scattering vector $g_{\varphi\psi}^{hkl}$ and the surface normal \mathbf{N} and an angle η , which describes the rotation around the scattering vector $g_{\varphi\psi}^{hkl}$ [41]

$$\sin \alpha = \sin \theta \cos \psi - \cos \theta \sin \psi \cos \eta, \quad (4)$$

$$\sin \beta = \sin \theta \cos \psi + \cos \theta \sin \psi \cos \eta. \quad (5)$$

Inserting $\eta = 0^\circ$ and 90° , respectively, yields the well-known expressions for the Ω - and Ψ -mode of XSA [42]. Taking into account the depth dependence of the residual strain/stress state, the fundamental equation of XSA becomes

$$\varepsilon_{\varphi\psi}^{hkl}(\tau) = \frac{1}{2} S_2^{hkl} \{ [\sigma_{11}(\tau) \cos^2 \varphi + \sigma_{22}(\tau) \sin^2 \varphi + \sigma_{12}(\tau) \sin 2\varphi] \sin^2 \psi + \sigma_{33}(\tau) \cos^2 \psi + [\sigma_{13}(\tau) \cos \varphi + \sigma_{23}(\tau) \sin \varphi] \sin 2\psi \} + S_1^{hkl} [\sigma_{11}(\tau) + \sigma_{22}(\tau) + \sigma_{33}(\tau)], \quad (6)$$

where S_1^{hkl} and $\frac{1}{2} S_2^{hkl}$ are the diffraction elastic constants (DEC). For bulk materials with $D \gg \tau$ (D — sample thickness) the correlation between the experimentally accessible lattice strain and the residual stress depth profiles $\varepsilon_{\varphi\psi}^{hkl}(\tau)$ and $\sigma_{ij}(\tau)$, respectively, and the real space depth profiles $\varepsilon_{\varphi\psi}^{hkl}(z)$ and $\sigma_{ij}(z)$ is given by the integral transformations [34]

$$\varepsilon_{\varphi\psi}^{hkl}(\tau) = \frac{\int_0^\infty \varepsilon_{\varphi\psi}^{hkl}(z) \exp(-z/\tau) dz}{\int_0^\infty \exp(-z/\tau) dz}, \quad (7)$$

$$\sigma_{ij}(\tau) = \frac{\int_0^\infty \sigma_{ij}(z) \exp(-z/\tau) dz}{\int_0^\infty \exp(-z/\tau) dz}. \quad (8)$$

Download English Version:

<https://daneshyari.com/en/article/5492512>

Download Persian Version:

<https://daneshyari.com/article/5492512>

[Daneshyari.com](https://daneshyari.com)